FEATURE ARTICLE

Anisotropic Metal Nanoparticles: Synthesis, Assembly, and Optical Applications

Catherine J. Murphy,* Tapan K. Sau, Anand M. Gole, Christopher J. Orendorff, Jinxin Gao, Linfeng Gou, Simona E. Hunyadi, and Tan Li

Department of Chemistry and Biochemistry, University of South Carolina, 631 Sumter Street, Columbia, South Carolina 29208

Received: April 2, 2005; In Final Form: May 6, 2005

This feature article highlights work from the authors' laboratories on the synthesis, assembly, reactivity, and optical applications of metallic nanoparticles of nonspherical shape, especially nanorods. The synthesis is a seed-mediated growth procedure, in which metal salts are reduced initially with a strong reducing agent, in water, to produce ∼4 nm seed particles. Subsequent reduction of more metal salt with a weak reducing agent, in the presence of structure-directing additives, leads to the controlled formation of nanorods of specified aspect ratio and can also yield other shapes of nanoparticles (stars, tetrapods, blocks, cubes, etc.). Variations in reaction conditions and crystallographic analysis of gold nanorods have led to insight into the growth mechanism of these materials. Assembly of nanorods can be driven by simple evaporation from solution or by rational design with molecular-scale connectors. Short nanorods appear to be more chemically reactive than long nanorods. Finally, optical applications in sensing and imaging, which take advantage of the visible light absorption and scattering properties of the nanorods, are discussed.

Introduction

Fine metal particles with nanometer-scale dimensions are of great interest due to their unusual properties.[1−3] Fundamentally, the mean free path of an electron in a metal at room temperature is ∼10−100 nm, and one would predict that as the metallic particle shrinks to this dimension, unusual effects should be observed.[1−3] Indeed, gold nanospheres of diameter ∼100 nm or smaller appear red (not gold) when suspended in transparent media,[1−3] and gold nanoparticles of diameter less than ∼3 nm are no longer "noble" and unreactive, but can catalyze chemical reactions.[4,5] In addition to favorable functional properties, nanometer scale metallic wires show extraordinarily high combinations of strength, stiffness, and ductility relative to bulk materials. Nanorods and nanowires have promising applications in electronics,[6,7] photonics,[8−10] hierarchical biologically inspired nanocomposites,[11−13] (bio)chemical sensing and imaging,[14,15] and drug delivery.[16,17]

The optical properties of silver and gold nanoparticles are tunable throughout the visible and near-infrared region of the spectrum as a function of nanoparticle size, shape, aggregation state, and local environment,[1−3,18−35] (Figure 1). Additionally, molecules adsorbed to the surface of gold and silver nanoparticles undergo enhanced surface-enhanced Raman scattering (SERS) effects, due to the coupling of the plasmon band of the irradiated metal (i.e., the collective oscillation of the conduction band electrons upon absorption in the visible for these particular metals, due to their dielectric constant) with the molecules' electronic states.[26−28] Thus, one emerging application of metallic nanoparticles is optical sensors, and single-molecule detection via SERS has been reported.[29,30]

For nanorods and nanowires, the plasmon band of the metal is split in two: the longitudinal plasmon band, corresponding to light absorption and scattering along the long axis of the particle, and the transverse plasmon band, corresponding to light absorption and scattering along the short axis of the particle.[18,24,25] (Additional weaker bands, corresponding to quadrupoles, may also be observed for nonspherical metal nanoparticles.[24]) Metallic nanorods and nanowires can have enhanced electric fields at the tips compared to spheres, which would lead to increased SERS activity.[24,31−33,35]

Gold colloids have been used for years as contrast agents in electron microscopy because gold is so electron-dense. More recently, gold and silver nanoparticles are used in biological optical imaging and sensing applications.[15,20,21,36−58] These nascent technologies rely in part on the excellent elastic light-scattering properties of metal nanoparticles,[15,41,53,57] and also on the shift of the plasmon band maxima with local dielectric constant.[41,52] Surface-enhanced fluorescence with metal nanoparticles is gaining attention as a way to detect molecules.[59−62] Surface-enhanced fluorescence bears some analogies to SERS, in that the spectral signal for a molecule is intensified by a nearby metal nanoparticle; but in the case of surface-enhanced fluorescence, an enhanced fluorescence signal occurs when the molecule is ∼10−100 nm away from the metal surface.[59−62] Theoretically, such surface-enhanced effects are larger for nanorods compared to nanospheres.[62] Even the thermal properties of unusually shaped metal nanoparticles are of interest to the biomedical community; for example, the large amount of near-IR light that gold nanoshells of appropriate size and shape

* To whom correspondence should be addressed: murphy@mail.chem.sc.edu.

10.1021/jp0516846 CCC: $30.25 © 2005 American Chemical Society
Published on Web 06/18/2005

Catherine J. Murphy is the Guy F. Lipscomb Professor of Chemistry at the University of South Carolina. She received BS degrees in chemistry and in biochemistry from the University of Illinois at Urbana-Champaign in 1986, where she performed undergraduate research in organometallic chemistry with T. B. Rauchfuss. She obtained a Ph.D. in inorganic chemistry from the University of Wisconsin in 1990, under the direction of Arthur B. Ellis. She was an NSF and NIH postdoctoral fellow at the California Institute of Technology from 1990 to 1993 in the laboratory of Jacqueline K. Barton. Since 1993 she has been on the faculty at South Carolina. Her research interests include the synthesis, characterization, and optical applications of inorganic nanomaterials; coordination compounds for optical sensing; and optical probes of local DNA structure and dynamics. She has won numerous research and teaching awards and sits on the editorial advisory board for seven journals.

Tapan K. Sau is an assistant professor in the Department of Chemistry at Panjab University, Chandigarh, India, and was on leave 2003−2004 to work in Catherine J. Murphy's laboratory as a postdoctoral research fellow. He obtained his Ph.D. from the Indian Institute of Technology in Kharagpur, under the direction of Tarasankar Pal. His research interests center on the synthesis and assembly of inorganic nanoparticles.

Anand M. Gole has been a postdoctoral research fellow in Catherine J. Murphy's group at the University of South Carolina since November, 2003. He obtained his Ph.D. degree from the National Chemical Laboratory, Pune, India, under the direction of Murali Sastry, and thereafter held a one-year postdoctoral fellowship at the Laboratoire de Physique des Solides, Orsay, France, before joining the University of South Carolina. His past and current research interests include synthesis, surface modification, organization and bioconjugation of inorganic nanoparticles and nanorods, studies on protein-lipid biocomposites, 2-D assembly of nano and biocomposites using various self-assembly techniques, polymer-surfactant and nanoparticle-lipid interactions on surfaces and interfaces.

Christopher J. Orendorff is a postdoctoral research fellow at the University of South Carolina. He earned his Ph.D. degree in analytical chemistry from the University of Arizona in 2003, under the direction of Jeanne Pemberton. His research interests include the optical properties of metallic nanorods/nanowires, the development of these materials as chemical and biological sensors, and the manipulation of nanorods/nanowires on substrates and in solutions.

Jinxin Gao is a recent (May 2005) Ph.D. graduate from Catherine Murphy's group at the University of South Carolina. His research interests are in surfactant-directed and dendrimer-directed synthesis of inorganic nanoparticles for catalytic applications.

Linfeng Gou is a senior graduate student in Catherine Murphy's group at the University of South Carolina. He graduated from Xi'an University of Architecture & Technology in China and joined the Murphy group in 2001, with a research focus on the synthesis of, and catalyts with, inorganic nanoparticles.

Simona E. Hunyadi is a second-year graduate student in Catherine Murphy's group at the University of South Carolina. She received a Bachelor of Science degree in 1995 from Babes-Bolyai University, Romania, in Chemistry with a minor in Physics. In 1996 she completed a Master of Science degree from Babes-Bolyai University in Chemistry with an emphasis in modified electrodes. From 1996 to 2000 she conducted research in the field of Applied Electrochemistry with Prof. I.C. Popescu. Her research interests include synthesis and functionalization of nanostructured materials that include core-shell nanoparticles, hollow materials, photonic materials, bimetallic colloids, and bioluminescent materials.

Tan Li is a first-year graduate student in Catherine Murphy's group at the University of South Carolina. He received his BS degree in chemistry in 2003 from Shandong University, China, and has been at South Carolina since 2004.

absorb can be dumped into the surroundings as heat, and should the surroundings be cancer cells, novel cancer therapies are possible.[63]

All of the promise of these future technologies, based on nanometer-scale inorganic solids, relies on the production of nanoparticles of controlled size, shape, and crystal structure, in reasonable quantities, and further ultimately requires (especially for some photonic and electronic applications) that these nanoparticles be rationally assembled. Enormous progress has been made in the synthesis of inorganic nanospheres; routinely, control over the diameter of nanoparticles leads to particle size distributions that are within 10% of the mean diameter, and frequently within 5%. Only since the mid-1990s and later have there been good synthetic methods to make nanoparticles of controllable size *and* shape (other than spheres).[18,64−79]

In this article, we highlight our own efforts to explore the synthesis, assembly, and optical properties of anisotropic metallic nanoparticles, particularly nanorods. We aim to understand the mechanism that produces anisotropic particles rather than spheres, in order to guide future synthetic efforts in this area. The assembly of nanorods in organized ways, spaced by a certain distance, is just beginning,[10,33,34,80−86] and there are fascinating opportunities for photonic devices based on ordered arrays of nanorods, in which light can be bent around corners.[9,10] The reactivity of nanorods, especially anisotropic reactivity at different positions on the nanorods,[86−90] can be explored to produce nanorods that have biocompatible coatings, and to produce "smart" nanorods that can recognize specific analytes. This feature article complements other recent *Journal of Physical Chemistry* review articles and feature articles on nanocrystals and their properties.[24,91−93]

"Green" Synthesis of Metallic Nanorods with Tunable Aspect Ratio

We have developed a seed-mediated growth method to make gold and silver nanorods and nanowires of controllable aspect ratio − up to a limit.[66−68,72,94−99] The basic approach is shown in Figure 2. The reactions take place in air, in water, at room temperature, and, in principle, are amenable to scaling up.

Metal salts are reduced in water, in air, at room temperature, with a strong reducing agent (sodium borohydride) to yield 3.5−4 nm spherical "seed" particles. These faceted nanospheres appear to be single crystalline[96] and can be capped with a variety of surface groups (citrate, surfactants, etc.) that could be present during the reaction. As the seeds "age," in order for any excess borohydride to react with water, growth solutions containing more metal salt, a structure-directing agent, and a weak reducing agent are prepared in a separate flask. The weak reducing agent is usually ascorbic acid (vitamin C), and by itself, at room temperature, is not capable of fully reducing the metal salt all the way to the elemental metal; but upon addition of the seeds, the reaction is thought to take place on the seed surface and be autocatalytic, to produce larger nanoparticles. The presence of the structure-directing agent is crucial to obtaining nanorods, as opposed to larger nanospheres; in our case, we have found that cetyltrimethylammonium bromide (CTAB) is uniquely suited to produce rods. More details on the mechanism will be explored below.

For reasons not presently understood, gold nanorods starting from ∼3.5−4 nm spherical seeds can grow out to 20−30 nm wide and up to 600 nm long, and no more. Aspect ratio, length divided by width, varies from ∼2 to ∼25 and is controlled by the relative concentrations of reagents. For silver, nanowires up to a dozen microns long can be made, with little control once the reaction takes off; these wires have a diameter within several nanometers of 30 nm.[66,102]

In exploring the influence of various synthetic parameters on nanorod production, we have examined both the nature of the seed and the concentrations of reagents in the growth steps.

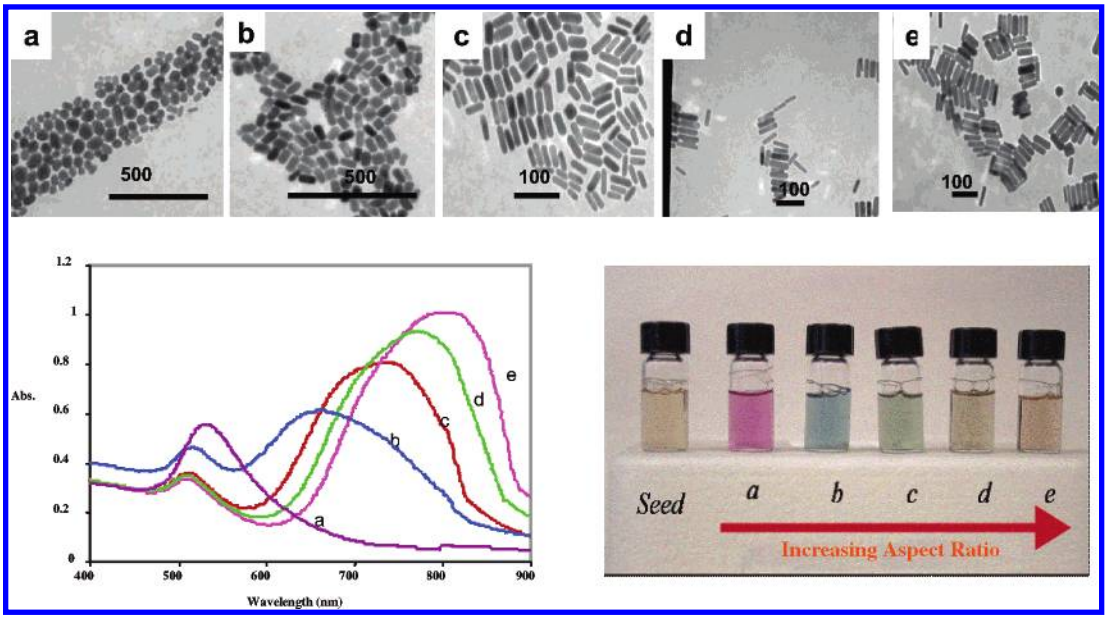

Figure 1. Transmission electron micrographs (top), optical spectra (left), and photographs of (right) aqueous solutions of gold nanorods of various aspect ratios. Seed sample: aspect ratio 1; sample a, aspect ratio 1.35 ± 0.32; sample b, aspect ratio 1.95 ± 0.34; sample c, aspect ratio 3.06 ±0.28; sample d, aspect ratio 3.50 ± 0.29; sample e, aspect ratio 4.42 ± 0.23. Scale bars: 500 nm for a and b, 100 nm for c, d, e.

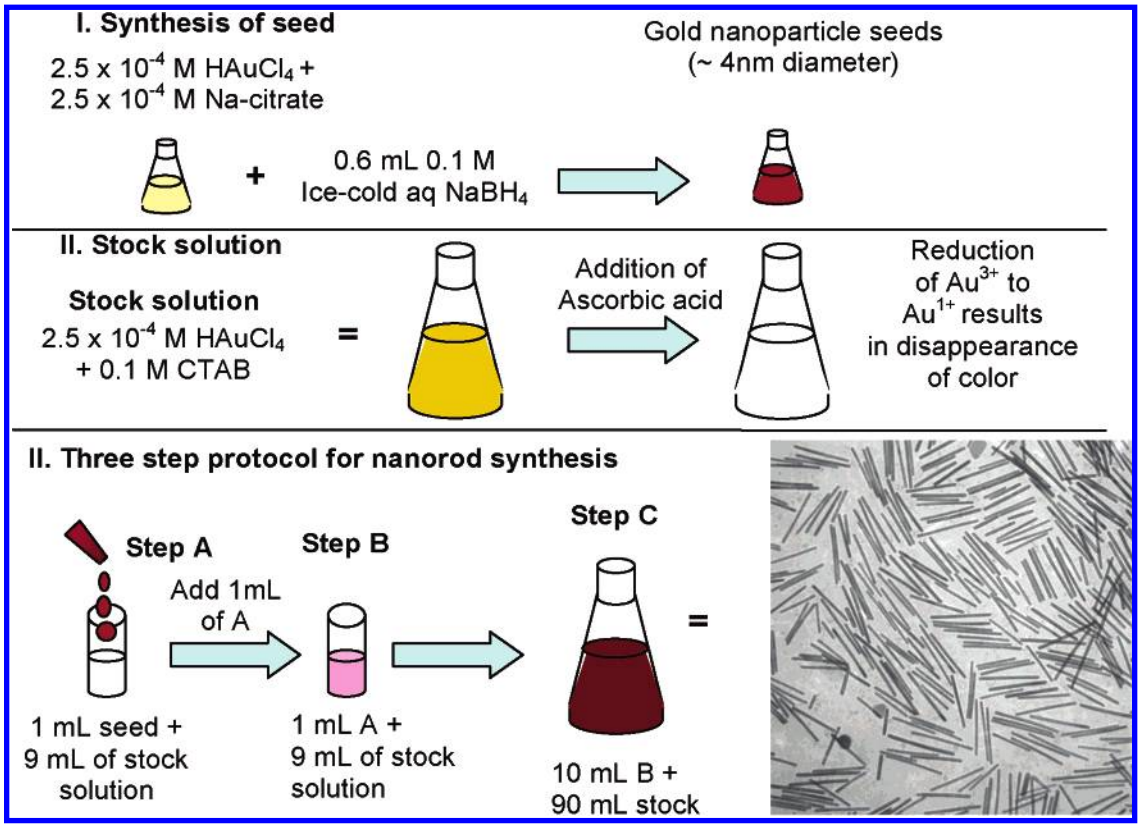

Figure 2. Seed-mediated growth approach to making gold and silver nanorods of controlled aspect ratio. The specific conditions shown here, for 20 mL volume of seed solution, lead to high-aspect ratio gold nanorods. (bottom right) Transmission electron micrograph of gold nanorods that are an average of 500 nm long.

We have discovered that smaller seeds, in general, produce higher-aspect ratio nanorods[99] (Figure 3).

The concentration of CTAB is critical for nanorod growth: 0.1 M concentrations are required, even though the critical micelle concentration for CTAB is far less than that. If CTAB were solely functioning as a soft rodlike micellar template for gold nanorod growth, this high concentration requirement is odd. The role of additive metal ions is also important for nanorod growth. For example, we have found that the presence of ~5% Ag^+ raises the yield of gold nanorods to nearly 100%, compared to ~20−40% in the absence of Ag^+.[72] However, the highest aspect ratio gold nanorods obtainable with silver ion is about 6, compared to ~25 in the absence of silver. Therefore, we obtain high yields of short gold nanorods in the presence of silver ion, but lower yields of longer gold nanorods without silver ions. In our reaction conditions, the concentrations of silver ion and bromide ion (from CTAB) are sufficiently high (0.1 M for CTAB) that AgBr precipitation should occur,

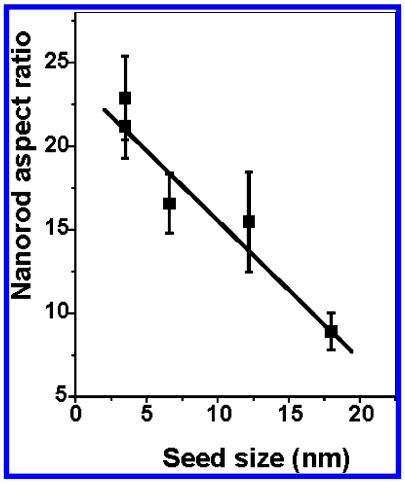

Figure 3. Experimental dependence of nanorod aspect ratio (vertical axis) on seed size. Gold nanorods were made using the seed-mediated protocols to obtain the highest aspect ratio nanorods for each seed size. Seeds were all anionic. The original data are from ref 99.

although we do not observe it on the macro scale. Therefore, we believe that AgBr might form monolayers in an epitaxial fashion[72] on the growing gold nanorod, and therefore inhibit growth at those faces. An additional complicating factor, however, is that slight changes in reaction conditions lead to other shapes, in high yield, of gold nanoparticles, including blocks, cubes, and tetrapods[98] (Figure 4).

These results suggest that these reaction products arise from kinetic effects rather than thermodynamic effects, and it appears, at least preliminarily, that these other shapes are not intermediates on the way to nanorods. We can certainly explore the effect of other metal ions on the growth of gold nanoparticles into interesting shapes; but in the absence of a rational understanding of how they might grow, all such experiments will be analogous to high-throughput screening, rather than rational design. We have already found, on the anion side, that bromide is crucial to making gold nanorods − cetyltrimethyammonium chloride as a structure-directing agent gives only spheres! Iodide as a counterion gives apparently random mixtures of shapes.

Crystallography of Metal Nanorods: Insight into the Growth Mechanism

It is imperative to understand the crystallography of metallic nanorods, prepared in the presence of metal ions, to understand the growth mechanism(s). For completeness, we also need to crystallographically characterize the shapes of other gold nanoparticles obtained under very similar reaction conditions (Figure 4). In particular, knowledge of the crystallography of both stable and metastable (relatively higher energy) nanorods can help to elucidate the overarching factors and local mechanisms leading to nanorod growth.

High aspect ratio (∼25) gold nanorods made by our seed-mediated growth approach with CTAB have already been examined by high-resolution transmission electron microscopy (HRTEM) and selected area electron diffraction (SAED)[96] (Figure 5). These rods were made without any additive metal ions. The end result was that the rods are pentatetradedral twins.[96] The cubic symmetry of the fcc lattice is broken by twinning.

Based on these data, which were collected and analyzed in collaboration with Stephen Mann, University of Bristol, UK, we postulated that the CTA^+ headgroup binds to the side surface with some preference (but not a great deal of preference, since many spherical products are obtained). The preferential binding is based on sterics − the Au atom spacing on the side faces is more comparable to the size of the CTA^+ headgroup than the close-packed {111} face of gold, which is at the ends of the nanorods. Such binding stabilizes the side faces, which have relatively large surface energy and stress (tension) compared to other faces. This allows material addition along the [110] common axis on {111} faces, which do not contain the CTA^+ headgroups. Other workers have found analogous crystallography for fcc metal nanorods.[69,103]

The results from the crystallographic analysis lead to the preliminary conclusion that the headgroup of the surfactant (or a complex ion version of it) is the primary director of nanoparticle shape. However, this preliminary conclusion is too simplistic. We have performed experiments in which we varied the tail length of the surfactant, keeping the cetyltrimethylammonium headgroup and the bromide counterion the same, and run the synthesis to produce the highest aspect ratio gold nanorods possible with a series of surfactants.[104] Were the headgroup the primary director, we would expect that the reactions would all produce aspect ratio ∼25 gold nanorods. Using 10-carbon, 12-carbon, and 14-carbon versions of CTAB (which has 16 carbons in the tail), we found that the tail length is surprisingly important (Figure 6).[104] As judged by FTIR and thermogravimetric analysis, the hydrophobic tails of CTAB interdigitate to make a bilayer on the rods,[100,105] with the cationic headgroup of the first monolayer facing the gold surface and the second layer's cationic headgroup facing the aqueous solvent.[100,105]

These data suggest that the formation of the presumed surfactant bilayer on the gold nanoparticles as they grow is quite important. All of these surfactants make rodlike micelles in water, with the critical micelle concentration decreasing with increasing tail length.[106] The tail contribution to the standard free energy of micellization for C_nTAB in aqueous solution has been estimated to be[106]

$$\Delta G^\circ = 2.303(2 - z/j)RT(0.1128 - 0.3074n) \qquad (1)$$

where n is the number of carbon atoms in the surfactant tail; z

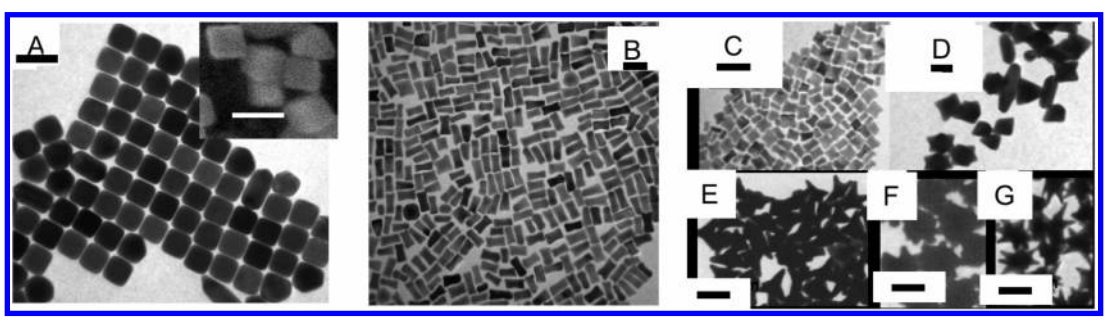

Figure 4. TEMs of gold nanoparticles of many shapes, all prepared with CTAB and in the presence of silver ion.[98] Scale bars are 100 nm for A, B, C, D; and 500 nm for E, F. G.

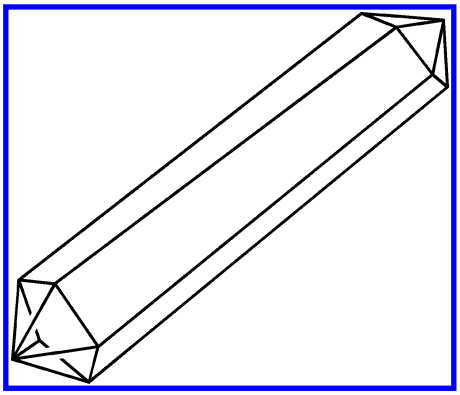

Figure 5. Cartoon of the crystallography of gold nanorods. The direction of elongation is [110]. The cross-sectional view is a pentagon; each end of the rod is capped with five triangular faces that are Au{111}. The sides of the rods are not as well-defined; either Au{100} or Au{110} faces, or both.

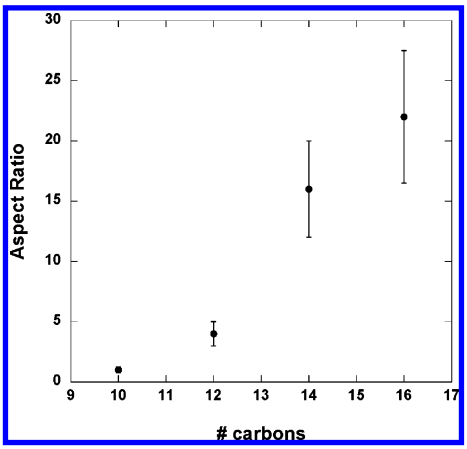

Figure 6. Dependence of gold nanorod aspect ratio on the tail length of the cationic surfactant CnTAB (all alkyltrimethylammonium bromides).

is the charge on the micelle; j is the aggregation number of the micelle; R is the gas constant, and T is temperature.

If we assume that the tail contribution to the free energy formation of a bilayer on gold is similar to that of micellization, and if we further assume that the z/j ratio is small compared to 2, we find that that $\Delta G^{\circ}_{n=10} = -29.6$ kJ/mol, $\Delta G^{\circ}_{n=12} = -35.8$ kJ/mol, $\Delta G^{\circ}_{n=14} = -41.9$ kJ/mol, and $\Delta G^{\circ}_{n=16} = -48.1$ kJ/mol. Thus, the free energy of bilayer stabilization between C_nTAB surfactants is approximately 6 kJ/mol per two methylene groups, which is much larger than RT (~2.5 kJ/mol). As a consequence, the dynamic formation of a bilayer of surfactant on gold surfaces via the hydrocarbon tails may indeed provide enough stabilization during gold nanorod growth, in a "zipper" fashion, to lead to the formation of longer nanorods for longer surfactant tails[104] (Figure 7).

More recently, experiments in which we vary the counterion of CTAB show that Br^- seems to be the most crucial piece; other workers have found too that anions play an enormously important role in nanocrystal growth.[74] Only with bromide, all other conditions remaining the same, do we obtain monodisperse rods, tetrapods, blocks, cubes, etc. In the case of shapes other than rods, silver ion (see above) is required. The K_{sp} for AgBr is 5.0×10^{-13} at room temperature. The metal ion absolute concentrations are 1−100 μM, bromide is 0.1 M in our experiments; thus, AgBr is likely to form under our conditions. The surface science literature suggests that bromide and silver bromide chemisorb on gold crystal faces.[107−111] Thus, bromide, or silver bromide, might be the initial species that deposit on the gold seed in our experiments. However, the affinity of bromide or silver bromide for gold is modest; therefore, high concentrations of bromide would be required to drive the ion onto the gold surface. If this notion is correct, then lowering the amount of CTAB in solution, which would lower the Br^- concentration, would favor spheres, which is indeed the case, since very high concentrations of CTAB are required to synthesize rods using our method.[66,67,94]

At this point, we can postulate a general mechanism of nanorod growth that might have reasonable predictive power. The mechanism may be relevant only to fcc metals. The mechanism starts with the single crystalline seed particles (Figure 8). Second, surface binding groups (surfactant, metal ions? halides? metal halide?) that may preferentially bind to certain crystal faces of the seed, or growing nanorod (or other shape) are present. CTAB alone in water makes spherical rodlike micelles, and originally it was thought that metal nanorods would grow due to CTAB being a soft template;[94] but in this mechanism, we suspect that CTAB directs the growth by blocking the long axis crystal faces, and so promoting metal growth on the short-axis faces[68,96] to make nanorods.

Mulvaney et al. has independently postulated an fcc metal nanorod growth mechanism which invokes the local electric field

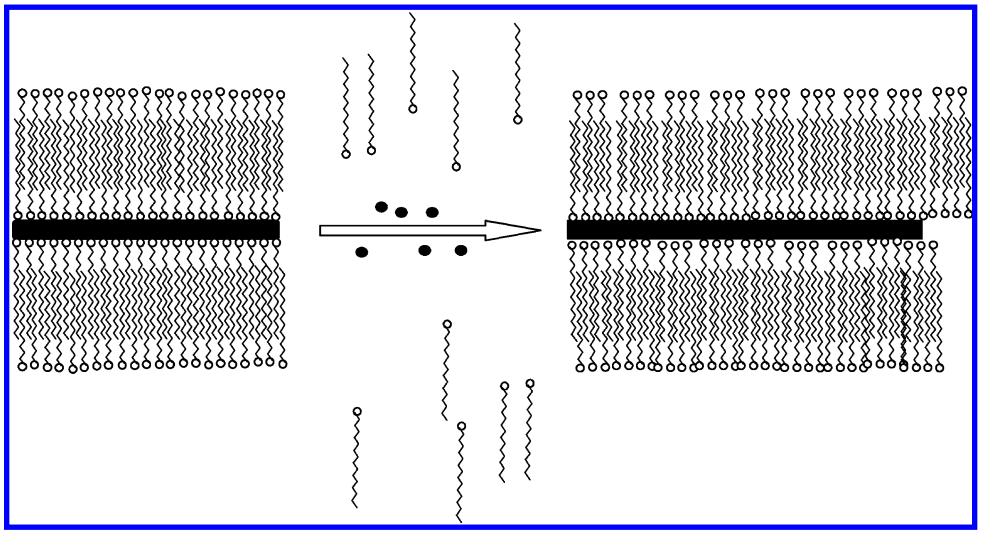

Figure 7. Cartoon illustrating "zipping": the formation of the bilayer of CnTAB (squiggles) on the nanorod (black rectangle) surface may assist nanorod formation as more gold ion (black dots) is introduced. Reproduced from ref 104 with permission.

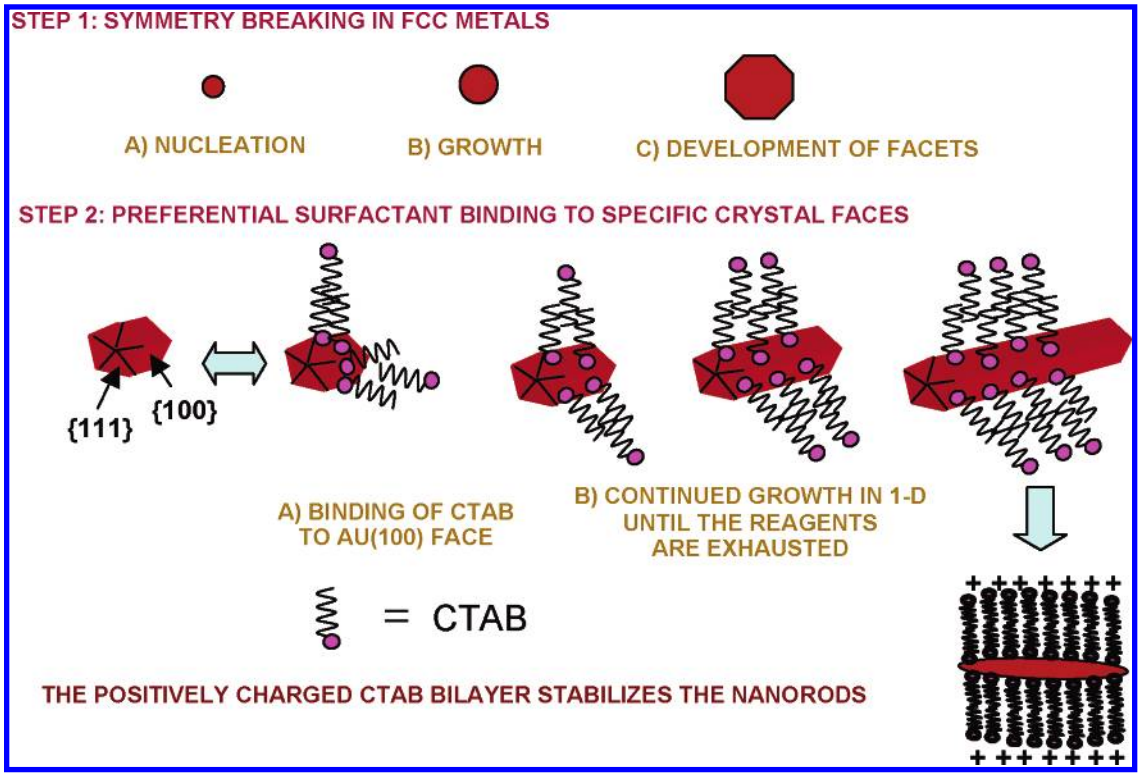

Figure 8. Proposed mechanism of surfactant-directed metal nanorod growth. The single crystalline seed particles have facets that are differentially blocked by surfactant (or an initial halide layer that then electrostatically attracts the cationic surfactant). Subsequent addition of metal ions and weak reducing agent lead to metallic growth at the exposed particle faces. In this example, the pentatetrahedral twin formation leads to Au {111} faces that are on the ends of the nanorods, leaving less stable faces of gold as the side faces, which are bound by the surfactant bilayer.

at the tips of growing nanorods and CTAB micelles.[112] Specifically, their model finds that Au(III) and Au(I) intermediates bind strongly to CTAB micelles, which are carried to the seed particles, and delivered preferentially at the tips to promote nanorods instead of nanospheres. One difficulty with this mechanism is the "tips" of the seeds − how do the seeds have tips initially? Mulvaney agrees:[112] "The model does not explain explicitly the initial change in morphology....It may be that a stacking faulty or twinning plane in the seed is also necessary to create an initial electric field asymmetry." Interestingly, recent molecular dynamics simulations of gold atoms made to form a nanorod show that the arrangement of the gold atoms relaxes substantially to change the nanorod crystallography.[113] This suggests that the twinning that occurs in the reaction mixture might lower the energy of the system to favor anisotropic shapes.

Our proposed mechanism suggests several features of the synthesis that can readily be checked. For example, the less stable the surfactant bilayer, the less tendency it will have to form a "blocking raft" on the growing nanorods, and the less likely it will be for anisotropic shapes to develop. This does seem to be true, based on the surfactant tail length study described above. This mechanism also implies that the surface energies of the initial seed are important, in the sense that binding of stabilizing ions to them winds up governing the final shape of the particle, and this in turn implies that large seeds, where the individual facets presumably have lower surface energies than the corresponding facets in smaller seeds, will not be as effective in promoting the formation of anisotropic shapes. This again appears to coincide with the results from the seed study described above; we found there, too, that larger seeds lead to a greater polydispersity in the final nanomaterials.[99] The mechanism also implies that if the CTAB bilayer, after its formation, could be destabilized (for example, by heating), then addition of metal ions and reducing agents might fatten the nanorods up instead of making them longer by favoring deposition of metal on the more abundant side faces of the rods. Preliminarily, in our lab, this appears to be the case as well.

However, our surfactant-directed approach is not the only possible one to generate nanorods and nanowires. For example, we have found that silver nanowires up to 10 μm long and 30 nm diameter, can be prepared from boiling aqueous solutions of silver nitrate, sodium hydroxide, and sodium citrate.[102] No seeds or surfactants are present! This suggests to us that small ions such as hydroxide can function as a structure-directing agent as well, to promote the growth of anisotropic crystals.[74,101]

Assembling Nanorods in One, Two and Three Dimensions: Surface Chemistry Is Key

One-dimensional, or end-to-end, assembly of metal nanorods is attractive for several applications. The electric field at the ends of nanorods, upon plasmon excitation, is calculated to be large and should be useful for surface-enhanced Raman or fluorescence sensing applications.[31,33,34,62] Nanoscale electronics require ordering of nanoscale metals.[6,7,65] With all long axes oriented in the same direction, a 1D array of metal nanorods would strongly absorb light of specific wavelengths (that are tunable with nanorod aspect ratio) with polarizations parallel to the rod axis − useful properties for photonic applications.[9,10] A number of groups are attempting to line up nanorods in one dimension by various self-assembly schemes.[114−116] We have found, unexpectedly, that biological linkers gave preferential end-to-end assembly of gold nanorods[86] (Figure 9). In those experiments, gold nanorods, aspect ratio ~20, prepared in the presence of CTAB, were exposed to an ethanolic solution of biotin disulfide for 24 h. This step presumably led to biotinylated nanorods. Upon addition of streptavidin, a protein that is well-known to tightly bind to one to four biotins, we expected to

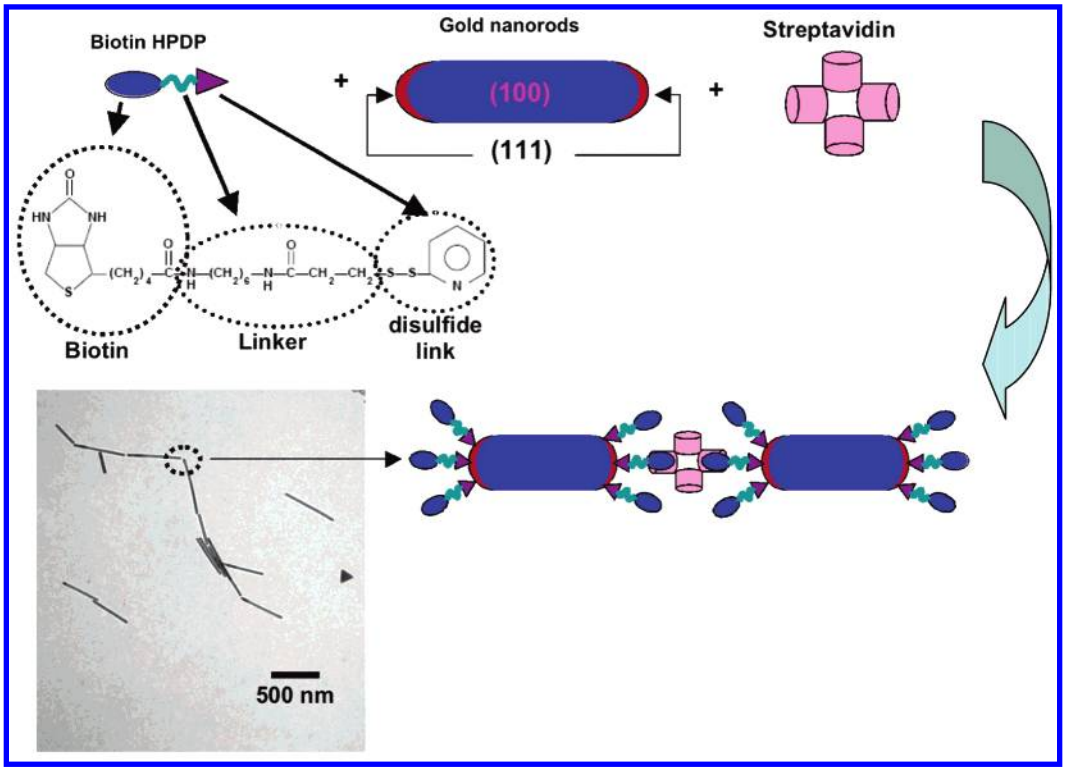

Figure 9. Cartoon of biotin-streptavidin assembly of gold nanorods; a biotin disulfide is added to biotinylate the rods, and subsequent addition of streptavidin causes noncovalent assembly. Inset: transmission electron micrograph of gold nanorod-streptavidin assemblies. The original data are from ref 86.

observe a precipitate or a large aggregate of gold nanorods, spaced in all three dimensions by the size of a streptavidin molecule (~5 nm). However, we observed no such objects; instead, the principle product was end-linked gold nanorods.

The mechanism was initially unclear, although two possibilities presented themselves. If the CTAB bilayer on the sides of the nanorods was not displaced by the biotin disulfide, then the biotin disulfide would preferentially make Au−S bonds at the ends of the rods, leading to linking via streptavidin preferentially at the ends. Another possibility was that the biotin disulfide did displace the CTAB, and made a self-assembled monolayer on the nanorod sides, which was too tightly packed for the protein to bind. Zeta potential measurements suggest that the nanorods remain highly positively charged after biotinylation. Biotin is a water-soluble neutral molecule; we would expect the net charge of the rods to decrease substantially if biotinylation of the rods was efficient. Therefore, we favor the model that leaves a CTAB bilayer on the sides of the rods and has biotin at the ends of the rods.

If the CTAB bilayer on the sides of the rods is indeed consistently difficult to displace (at room temperature), then bifunctional linker molecules, in principle, should link rods end-to-end. There is at least one report that this strategy works for hydrogen-bonding molecules,[116] but so far we have been unable to obtain reproducible results with many simple bifunctional molecules (e.g., $HS(CH_2)_nSH$). Based on the success of the biotin-streptavidin linkers, we propose that bulky linkers would be superior to molecules such as simple long-chain dithiols; the nanorod diameter is ~20−30 nm, and an additional ~6 nm layer is due to the bilayer of CTAB. Thus, molecules that are simple linear chains might not be enough "glue" to stick the nanorods together at the ends, especially since the ends are not flat, but terminate in the pentatetrahedral twin.[96] Solution conditions such as relative concentrations of reagents, pH, and ionic strength will all affect the nanorod assembly, especially if the linking strategy relies on electrostatics. Characterization of nanorod assembly is best performed by electron microscopy, light scattering (for average particle size in solution), and UV−vis spectroscopy (for aggregation changes/local dielectric constant effects). For end-to-end assembly, the longitudinal plasmon band of the nanorods will red shift significantly.[34,116]

An alternative strategy for one-dimensional alignment of metallic nanorods is to use physical methods such as stretching a polymer film containing the nanorods,[114] application of electric fields to films containing the nanorods,[117] or rubbing a substrate in one direction, followed by nanorod deposition. These methods are used with success to align liquid crystals,[118] and there is one paper that reports gold nanorod alignment by stretching of a film.[114] There is no good control over inter-nanorod distances in these methods, but nanorod alignment should be readily observable by atomic force microscopy on flat substrates, polarized absorption experiments on thin transparent films,[114,117] or by darkfield microscopy[21,22,24,41,53,57,77,119−121] on thin transparent films. In the latter technique, the Rayleigh-scattered light from unaligned rods will be various colors that correlate with the various angles the rods have with the view normal to the surface;[122] but upon alignment, the spots in the darkfield microscope ought to red shift as the long axis view of the nanorods becomes dominant.[72]

Recent exciting work in nanophotonics suggests that metal nanorods, organized side-by-side in two dimensions at a well-defined spacing, are excellent at propagating light down the nanorod chain, including around corners.[9,10] The optimal nanorod−nanorod distance for coupling plasmons, center-to-center, is 3 nanorod diameters, or 1 nanorod radius, between the surfaces of the nanorods.[123] For an aspect ratio of 4, e.g., nanorods that are 25 nm wide and 100 nm long, this corresponds to an inter-nanorod distance of 12 nm. In these photonic waveguide experiments, nanoparticles were made lithographically. A more versatile alternative would be to create self-

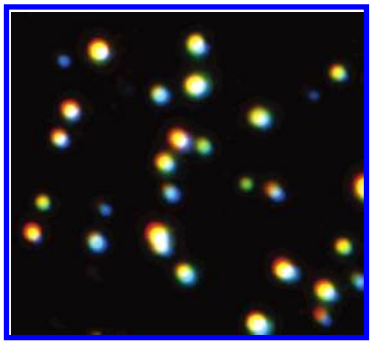

Figure 10. Dark field microscopic image of individual silver nanoparticles of various shapes. The field of view is ~1 mm; the spot size of the scattered light is far larger than the true size of individual nanoparticles. The different colors are due to the different nanoparticle shapes and orientations.

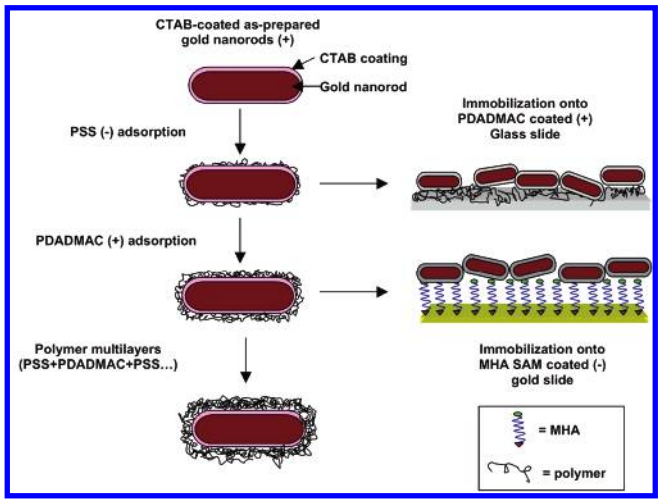

Figure 11. Cartoon of layer-by-layer deposition of polymers via electrostatic interactions onto gold nanorods, followed by fixing to a complementary surface. Taken from ref 126 with permission.

assembled structures of nanorods that could be deposited on a surface and have tunable spacing.

We have found that simple concentration of nanorod solutions leads to preferential side-to-side assembly.[85] This process is entropically driven, in part by release of water and counterions from the interface of adjacent nanorods.[124] Other shapes of gold nanoparticles can also be assembled to give organized arrays by a similar means.[105] In all of these cases, the presence of the CTAB appears to be crucial: it acts as molecular "glue" to assist in the organization, either by sharing common layers of counterions or by interdigitation of the hydrophobic tails from adjacent nanoparticles.[105]

The CTAB on the surface of the nanoparticles can be coated over with other molecules. In our case we have found that this works well using polyelectrolyte layer-by-layer techniques that others have successfully used for nanospheres.[125,126] For example, poly(diallyldimethylammonium chloride) (PDADMAC) is cationic at neutral pH, and poly(sodium-4-styrenesulfonate) is anionic: subsequent coating of CTAB-coated gold nanorods with PSS, then PDADMAC, PSS, etc., produces nanorods that appear larger and larger in light-scattering experiments, and flip their effective surface charge (zeta potential) from cationic to anionic as the polymers adsorb (Figure 11). Favorable electrostatic interactions can also be used to fix charged nanoparticles onto appropriately functionalized surfaces (Figures 11 and 12).

We have also found that other side-by-side assemblies of shorter gold nanorods can also be prepared in a pH-dependent manner.[127] In these experiments short gold nanorods, capped with the cationic CTAB bilayer, are incubated with adipic acid ($HOOC(CH_2)_4COOH$). At pH values below the pK_a of the carboxylic acid, no particular assembly of nanorods is observed (Figure 13), but at pH 7−8, the deprotonated adipic acid acts as a short rigid bridge between nanorods. In solution, light scattering experiments suggest that only small aggregates are formed,[127] but upon examination under the electron microscope extensive side-by-side assembly is observed.[127]

Three-dimensional assembly of nanoparticles − crystallization or superlattice formation − has been readily observed for spheres.[95,128] DNA linkers have been found to assemble nanorods in all three dimensions.[129] Characterization of three-dimensional assemblies is more difficult and is primarily performed by electron microscopy to measure inter-rod distances.[130]

Reactivity of Metallic Nanorods: Core−Shell Materials

Gold and silver, as noble metals, are relatively unreactive in the bulk. However, the metals can undergo complex ion formation that leads to metal dissolution. For example, gold is purified from ores by reaction with aqueous cyanide in air:[131]

$$4Au(s) + 8CN^-(aq) + 2H_2O(l) + O_2(g) \rightarrow 4[Au(CN)_2]^-(aq) + 4OH^-(aq) \quad (2)$$

Industrially, the gold is reduced back to the element with zinc dust.[131] Silver undergoes complex formation with ammonia to $[Ag(NH_3)_2^+]$ in an analogous reaction.[132] Do these reactivities depend on metal particle size and shape?

We have performed a series of cyanide reactions on gold nanorods of aspect ratio ~2 and ~20, per eq 2.[133] We found that short nanorods reacted much faster than long nanorods and that short nanorods preferentially reacted at the ends, to round down to spheres. However, we found that long nanorods took a surprisingly long time to dissolve compared to short rods (24 h at least, compared to about 30 min for short rods), and the reaction occurred more at the long faces of the rods rather than the ends. This observation runs somewhat counter to our studies that showed that these same long nanorods preferentially reacted at the ends in the case of biotin-streptavidin.[86]

Low aspect-ratio silver nanorods are unstable on the time scale of minutes in air and in light, presumably because of a photooxidation process that releases Ag^+. However, silver nanowires that are 30 nm in diameter, but up to a dozen microns long, are very stable under these conditions and indeed can be made from boiling water solutions in air and in light.[102] In our hands, gold nanoparticles of many different shapes are far more stable than silver, especially after purification from the reaction mixture. El-Sayed has discussed laser heating and melting of metallic nanorods.[19]

In addition to exploring the dissolution of the metal, we have also explored reactions at the nanorod surface in which the reactants made a covalent network shell around the nanorod core. As mentioned above, simple thiol-based reactivity of gold nanorods suggests that the ends are far more accessible than the sides of the rods: witness the preferential biotinylation at the nanorod ends, in the presence of the side-bound surfactant. However, in principle the CTAB bilayer should be more easily removed if covalent bonds are formed from an incoming reactant to make a covalent shell. An additional advantage of core−shell materials is that the nanorods will again have a new surface that can change their solubility, or decrease their propensity to salt out (from the native CTAB bilayer).

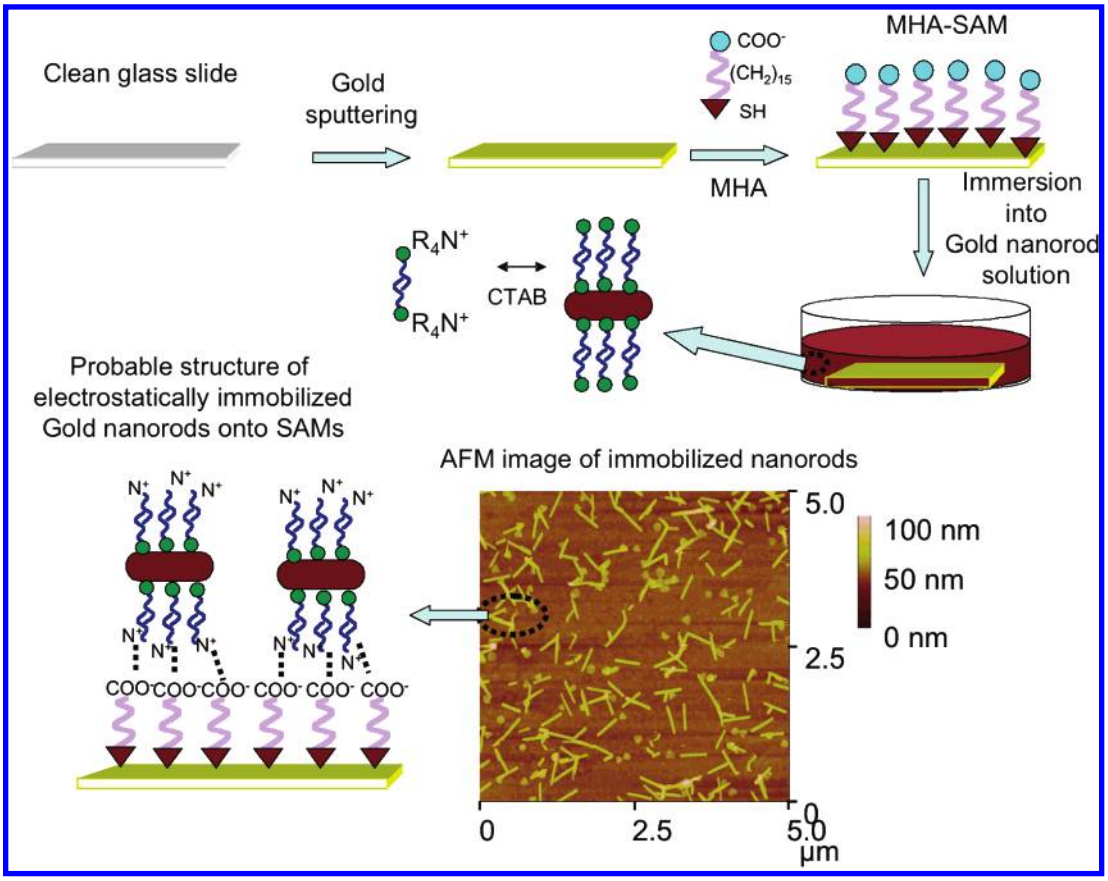

Figure 12. Cartoon showing the preparation of a self-assembled monolayer of mercaptohexanoic acid (MHA) on a flat gold substrate, subsequent immersion into an aqueous solution of CTAB-capped gold nanorods at a pH greater than 6 (so that the acid group is deprotonated), and final immobilization of the nanorods on the surface, governed by electrostatic interactions. Also shown is an atomic force microscopy image of nanorods immobilized in this fashion; field of view, 5 μm.

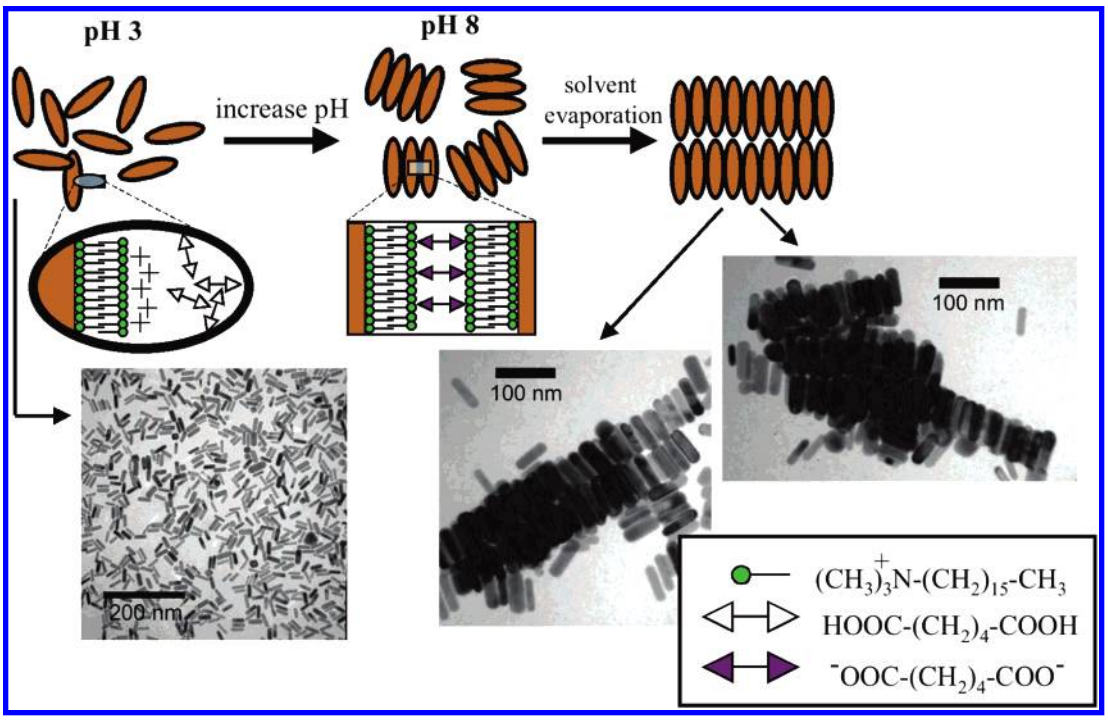

Figure 13. CTAB-capped gold nanorods are assembled side-by-side as a function of pH in the presence of adipic acid.[127] Monofunctional acids and long-chain diacids are not effective in analogous assembly reactions.[127]

Silica is a popular choice to coat nanoparticles.[132,134−137] Our group[138] has used a bifunctional linker, 3-mercaptopropyltrimethoxysilane (MPTMS), as a precursor in the silica coating process. MPTMS binds to a silver or gold surface through the thiol (Figure 14), leaving the trimethoxysilane group available for subsequent reaction with sodium silicate, to make SiO_2. Fortunately, the coated nanorods and nanowires remained as well-dispersed suspensions during the entire process of silica

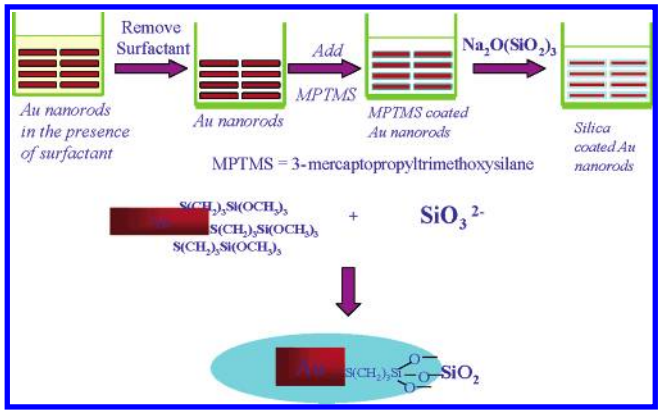

Figure 14. Excess CTAB surfactant is removed from nanorods by centrifugation and washing. MPTMS is added, followed by sodium silicate, to make SiO_2-coated nanorods.

coating, and there was no aggregation between the nanorods and nanowires.

The silica coating had a uniform thickness over the entire surface of each nanoparticle, including both ends. The thickness of the silica coat can be controlled with reaction time and reagent concentrations. The lengths of these nanocables were mainly determined by the specific template and can be as long as 14 μm in the case of Ag. The original morphology of each type of silver and gold nanostructure is essentially preserved in this surface-coating process.

The position of the plasmon peaks of metal nanoparticles is sensitive to the local dieletric constant.[18,21−25] The absorbance peaks for gold and silver functionalized with silica is red shifted compared to the original solutions, consistent with this notion.[138]

The metal core can be dissolved away with cyanide (for gold) or ammonia (with silver) to produce hollow silica nanotubes.[138] Thus, metal nanoparticles of various shapes are not only interesting in their own right but may be used as templates to make hollow structures of the coating material.[75,138]

We can control silica shell thickness, which is straightforward by controlling reagent concentrations and reaction conditions. Silica shells from ∼5 nm to ∼150 nm thick have been prepared. This is the thickness range over which we might expect to observe surface-enhanced fluorescence and other molecular fluorescence effects[62,139] from molecules that are near, but not too near, a nanoscale metal surface.

The surface modification of nanoparticles that have more exotic shapes, such as tetrapods, stars, etc., should in principle be doable; but to date, few papers have appeared on this topic, most likely because there are few methods to make such exotic shapes of nanoparticles in high yield.[87]

Optical Properties of Metallic Nanorods and Nanowires: Chemical Sensing and Imaging

Just as in bulk metals, electrons in the conduction band of nanoscale metals are free to oscillate upon excitation with incident radiation, referred to as the localized surface plasmon resonance (LSPR).[140] However, for metals on the nanoscale, the oscillation distance is restricted by the nanoparticle size. For gold and silver nanoparticles, LSPR corresponds to photon energies in the visible wavelength regime, giving rise to significant interest in their optical properties.[24,25,78,141,142] These optical characteristics include strong plasmon absorption, resonant Rayleigh scattering, and localized electromagnetic fields at the nanoparticle surface.

Plasmon absorption in metal nanoparticles is highly dependent on nanoparticle shape, size, and dielectric constant of the surrounding medium.[1] Figure 1 shows absorption spectra for gold nanorods of various aspect ratios. Spherical silver and gold nanoparticles have single plasmon absorption bands at ∼400 and ∼520 nm, respectively, that are relatively independent of size. Anisotropic gold and silver nanorods have two principle plasmon absorption peaks; one at shorter wavelength corresponding to absorption and scattering of light along the short axis of the nanorod (transverse plasmon band), and the other band at longer wavelength corresponding to absorption and scattering of light along the long axis of the nanorod (longitudinal plasmon band). The longitudinal plasmon absorption bands are tunable with nanorod aspect ratio from the visible to the near-IR.[1−3,18−35] Many excellent articles that describe the theoretical aspects of metal plasmons are available.[21−25]

Strong plasmon absorption and sensitivity to local environment have made metal nanoparticles attractive candidates as colorimetric sensors for analytes including DNA, metal ions, and antibodies.[143−145] These visible color changes are due to metal nanoparticle aggregation, which in turn affects the plasmon coupling and induced dipoles.[146−148] We have reported the use of gold nanoparticles as selective sensors for Li^+.[44] This solution-based sensor utilizes nanoparticles functionalized with a ligand that binds to gold via a thiol at its back end, and a phenanthroline derivative at the front end to selectively bind to Li^+ as a bidentate ligand. This Li^+ binding aggregates nanoparticles and gives a linear response of color shift with ion concentration.[44]

Resonant Rayleigh scattering from metallic nanoparticles is a unique characteristic of nanoscale metals.[21,149] There have been numerous reports on utilizing resonant Rayleigh scattering from gold and silver nanoparticles, made by colloidal or lithographic techniques, for biological and chemical analyses.[21,41,43,57,78,149] This stems from the sensitivity of these plasmon resonant particles (PRPs) to local chemical environment, refractive index, and nanoparticle size and shape.[22,120] An increasing number of reports are appearing in which the elastic light scattering from metallic nanoparticles is measured to infer nanoparticle position, local environment, or (in the case of nanorods) relative orientation.[21,41,43,57,78,149] We have reported the size dependence of light scattering from gold nanorods,[72] where the observed light scattering from gold nanorods red-shifts, on average, with increasing aspect ratio.

Figure 15 shows light scattering images of gold nanoparticles of various shapes taken in a dark field optical microscope. The inset in each of these images shows a TEM image of each nanoparticle. Dark field light scattering images were acquired using a Nikon L-150 reflective light source optical microscope with a BF/DF LU Plan 100× objective and a Micropublisher 5.0 digital camera. As reported for silver nanoparticles,[22,120] light scattering from gold nanoparticles is shape and size dependent.

The excellent light-scattering properties of gold nanorods are sensitive to their orientation.[122] We are currently using the polarized light scattering from short gold nanorods, aspect ratio 4, to determine nanorod orientation in polymer films. In this unpublished work, nanorods are incorporated into poly(vinyl alcohol) films and aligned by stretching the polymer. Observed light scattering shifts from green to red as the orientation of the stretch polymer is rotated 90°, corresponding to scattering from the transverse and longitudinal axes, respectively. We are beginning to use the light scattering from longer gold nanorods, aspect ratio 16, as pattern markers to determine strain in polymeric materials, for which individual "pixels" of nanorods serve as data points to track deformation. Other workers have used dark field microscopy to image nanoparticle uptake by

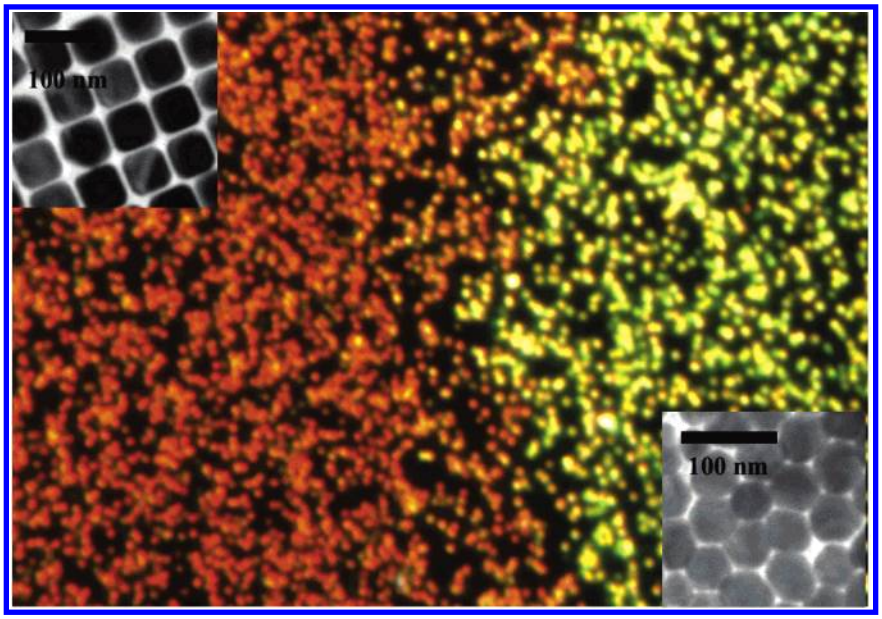

Figure 15. Dark field microscopy image of gold nanocubes (left) and gold "nanohexagons" (right), taken on solutions dried down on a microscope slide. The field of view is ~1 mm. Insets: transmission electron micrographs of the nanoparticles, scale bars = 100 nm.

cells[57] and have combined dark field microscopy with the LPSR shifts associated with local dielectric constant changes to have "light scattering biochips" for analyte detection.[41]

Inelastic visible light scattering from metal nanoparticles is also a useful means to gain chemical information about the nanoparticle's environment. Surface-enhanced Raman scattering (SERS) is a powerful analytical tool for determining chemical information for molecules on metallic substrates on the 10−200 nm size scale.[26−28] Raman vibrations of molecules are in general very weak; but in the presence of metals (copper, silver, gold) with nanoscale roughness, the molecular Raman vibrations excited by visible light are enhanced by orders of magnitude.[26−28] In general, there are two traditional operational mechanisms to describe the overall SERS enhancement: the electromagnetic (EM) and chemical (CHEM) enhancement mechanisms. EM enhancement is due to the increased local electric field incident on an adsorbed molecule at a metallic surface, due to visible light absorption by the metal. CHEM enhancement results from electronic resonance/charge transfer between a molecule and a metal surface, which leads to an increase the polarizability of the molecule.[26−28] Since the introduction of the SERS phenomenon on roughened silver electrodes, much attention has turned to SERS on spherical colloidal substrates of either gold or silver. Colloidal nanoparticles are of interest as SERS substrates not only because they are strong light scatterers but also because of their tunable optical properties, which depend on nanoparticle size, shape, and aggregation state, as described above. The largest surface enhancements, that seemingly lead to single molecule SERS, are observed for molecules adsorbed in the fractal space at junctions between nanoparticles, referred to as "SERS hot spots".[29,30] This is a result of localized surface plasmon (LSP) coupling between nanoparticles and the enhanced electromagnetic field intensity localized at nanoparticle junctions.[150−155]

Anisotropic metallic nanoparticles have all of the characteristics that make them excellent candidates as SERS substrates. Plasmon absorption bands can be tuned with nanocrystal aspect ratio to be in resonance with common visible laser sources, optimizing the EM enhancement mechanism. Moreover, anisotropic nanocrystals have highly curved, sharp surface features with dimensions less than ~100 nm. This can increase the local electric field up to 100-fold at the tip, referred to as the "lightning rod" effect.[156,157] Despite the desirable characteristics of metallic nanorods or other anisotropic as SERS substrates, only a few reports exist for SERS on rod- or wire-shaped nanoparticles.[158−162]

Recently, we have investigated the relationship between the SERS enhancement factor (the degree to which the metal nanoparticle increases the Raman signals of adsorbed molecules) and excitation resonance with longitudinal plasmon absorption for gold and silver nanorods.[163] Enhancement factors were determined for 4-aminothiophenol, 4-mercaptopyrine, and 2,2-bipyridine adsorbed to silver and gold nanorod colloidal substrates in aqueous solutions. These experiments were carried out at sufficiently dilute conditions so that aggregation effects and LSP coupling could be neglected. Our results[163] suggest that molecules adsorbed to substrates that have plasmon absorption in resonance with the excitation source show 10−100-fold greater SERS enhancement than those adsorbed to gold or silver nanoparticles in the off-resonance condition.

In addition to studying the effect of nanorod aspect ratio on SERS, we have also investigated the nanoparticle shape dependence on SERS in a sandwich geometry.[164] In this geometry, SERS substrates are prepared by electrostatically immobilizing CTAB-protected nanoparticles onto self-assembled monolayers of 4-mercaptobenzoic acid on smooth planar gold substrates. Observed SERS enhancements of the immobilized 4-mercaptobenzoic acid are attributed to a convolution of nanoparticle properties, plasmon absorption, and sharpness of features, and the well-documented coupling between nanoparticle localized surface plasmon (LSP) and the planar gold substrate surface plasmon polariton (SPP).[165−167] LSP−SPP coupling has been utilized previously to enhance signals in surface plasmon resonance spectroscopy (SPR) of biological samples in the same sandwich geometry.[168−170] Taking all factors into account, it appears that the nanoparticles with the most sharp corners and edges produce the largest SERS enhancements.[164] Gold nanospheres, immobilized on top of the 4-mercaptobenzoic acid monolayers, yielded an SERS enhancement factor of 10^7, while other anisotropic shapes had enhancement factors of 10^8−10^9.[164]

In addition to SERS, surface enhanced fluorescence has also been reported for molecules near the surfaces of metallic

nanoparticles.[59−62] While molecular fluorescence is quenched within ∼5 nm of the metal nanoparticle surface, at distances of ∼10 nm or greater, fluorescence is enhanced up to 100-fold by the localized electric field and increased intrinsic decay of the fluorphore.[59−62] However, surface-enhanced fluorescence using gold or silver nanorods or nanowires has not been reported and would seem to be a useful starting point for yet another optical sensing application for metallic nanoparticles.

Summary and Future Directions

Synthetic approaches to making gold and silver nanoparticles abound. We have been fortunate in that the initial choice of our surfactant, CTAB, turned out to have key features necessary for controlling gold and silver nanoparticle shape: it is highly water-soluble, has bromide counterions which can chemisorb on those metal surfaces, a sufficiently large headgroup to help direct which face of the crystal grows, and a sufficiently long tail to make a stable bilayer on the metal surface. Given that many ions and polymers are now being found to direct nanocrystal growth, there may be enough empirical data to start figuring out the design rules for growth (nucleation still being a mysterious phenomenon). However, in order for this to be done properly, the crystallography of all of these anisotropic shapes need to be determined for different reaction conditions, if epitaxial or relative surface-energy arguments are to be made as to which faces grow and which do not. This need for atomic-level imaging of nanoparticles then requires sufficient capabilities in high-resolution transmission electron microscopy, particularly with Z-contrast imaging to be able to perform elemental analysis on the near-atomic scale. For practicality in the marketplace, syntheses need to be scaled up to kilograms or more − a major challenge when milligrams of product are the norm.

There are many applications of metal nanoparticles that require their assembly on surfaces or aggregation in solution. Surface chemistry here is critical and is an active area of study. Less familiar to chemists, but more familiar to physicists, are issues of mechanical strain or stress that facets on nanoscale metal crystals might experience, which in turn have an impact on how structurally or chemically reactive a surface is. Bulk single crystalline surfaces are well-known to reconstruct; to what extent does this happen on nanoparticle surfaces? Molecular dynamics simulations, relatively scarce for nanomaterials, may prove illuminating for helping answer questions such as this.

The plasmon bands that gold and silver nanoparticles show in the visible region of the electromagnetic spectrum afford many excellent opportunities for photonics, chemical and biochemical sensing, and imaging applications. We have only touched on several possibilities here. But as the ability to make and modify nanocrystals continues to improve, the creative uses of these materials are sure to increase.

Acknowledgment. We thank the University of South Carolina, the National Science Foundation, the National Institutes of Health, and the USC NanoCenter for financial support of our metal nanoparticle work. We also thank our many colleagues and collaborators who gave generously of their time, expertise, and facilities to assist us with our experiments.

References and Notes

(1) El-Sayed, M. A. *Acc. Chem. Res.* **2001**, *34*, 257−264.
(2) *Metal Nanoparticles: Synthesis, Characterization and Applications*; Feldheim, D. L., Foss, C. A., Jr., Eds.; Marcel Dekker: New York, 2002.
(3) Daniel, M.-C.; Astruc, D. *Chem. Rev.* **2004**, *104*, 293−346.
(4) Valden, M.; Lai, X.; Goodman, D. W. *Science* **1998**, *281*, 1647−1650.
(5) Chen, M. S.; Goodman, D. W. *Science* **2004**, *306*, 252−255.
(6) Huang, Y.; Duan, X.; Lieber, C. M. *Science* **2001**, *291*, 630−633.
(7) Mallouk, T. E.; Kovtyukhova, N. I. *Chem. Eur. J.* **2002**, *8*, 4354−4363.
(8) Law, M.; Sibuly, D. J.; Johnson, J. C.; Goldberger, J.; Saykally, R. J.; Yang, P. *Science* **2004**, *305*, 1269−1273.
(9) Maier, S. A.; Brongersma, M. L.; Kik, P, G.; Meltzer, S.; Requichia, A. A. G.; Atwater, H. *Adv. Mater.* **2001**, *13*, 1501−1505.
(10) Maier, S. A.; Kik, P. G.; Atwater, H. A.; Meltzer, S.; Harel, E.; Koel, B. E.; Requichia, A. A. *Nature Mater.* **2003**, *2*, 229−232.
(11) Fan, H.; Lu, Y.; Stump, A.; Reed, S. T.; Baer, T.; Schunk, R.; Perez-Luna, V.; Lopez, G. P.; Brinker, C. J. *Nature* **2000**, *405*, 56−60.
(12) Gao, H. J.; Ji, B. H.; Jager, I. L.; Arzt, E.; Fratzl, P. *Proc. Natl. Acad. Sci. U.S.A.* **2003**, *100*, 5597−5600.
(13) Ji, B. H.; Gao, H. J. *J. Mech. Phys. Solids* **2004**, *52*, 1963−1990.
(14) Katz, E.; Willner, I. *Angew. Chem., Int. Ed. Engl.* **2004**, *43*, 6042−6108 [Epub ahead of print].
(15) Schultz, D. A. *Curr. Opin. Biotechnol.* **2003**, *14*, 13−22.
(16) Salem, A. K.; Searson, P. C.; Leong, K. W. *Nature Mater.* **2003**, *2*, 668−671.
(17) Tkachenko, A. G.; Xie, H.; Coleman, D.; Glomm, W.; Ryan, J.; Anderson, M. F.; Franzen, S.; Feldheim, D. L. *J. Am. Chem. Soc.* **2003**, *125*, 4700−4701.
(18) Hornyak, G. L.; Patrissi, C. J.; Martin, C. R. *J. Phys. Chem. B* **1997**, *101*, 1548−1555, and references therein.
(19) Link, S.; El-Sayed, M. A. *J. Phys. Chem. B* **1999**, *103*, 8410−8426.
(20) Elghanian, R.; Storhoff, J. J.; Mucic, R. C.; Letsinger, R. L.; Mirkin, C. A. *Science* **1997**, *277*, 1078−1080.
(21) Schultz, S.; Smith, D. R.; Mock, J. J.; Schultz, D. A. *Proc. Natl. Acad. Sci. U.S.A.* **2000**, *97*, 996−1001.
(22) Mock, J. J.; Barbic, M.; Smith, D. R.; Schultz, D. A.; Schultz, S. *J. Chem. Phys.* **2003**, *116*, 6755−6759.
(23) Kottman, J. P.; Martin, O. J. F.; Smith, D. R.; Schultz, S. *Chem. Phys. Lett.* **2001**, *341*, 1−6.
(24) Kelly, K. L.; Coronado, E.; Zhao, L. L.; Schatz, G. C. *J. Phys. Chem. B* **2003**, *107*, 668−677.
(25) Sosa, I. O.; Noguez, C.; Barrera, R. G. *J. Phys. Chem. B* **2003**, *107*, 6269−6275.
(26) Garrell, R. *Anal. Chem.* **1989**, *61*, 401A−411A.
(27) Campion, A.; Kambhampati, P. *Chem. Soc. Rev.* **1998**, *27*, 241−250.
(28) Kneipp, K.; Kneipp, H.; Itzkan, I.; Dasari, R. R.; Feld, M. S. *Chem. Rev.* **1999**, *99*, 2957−2975.
(29) Nie, S.; Emory, S. R. *Science* **1997**, *275*, 1102−1106.
(30) Jiang, J.; Bosnick, K.; Maillard, M.; Brus, L. *J. Phys. Chem. B* **2003**, *107*, 9964−9972.
(31) Imura, K.; Nagahara, T.; Okamoto, H. *J. Am. Chem. Soc.* **2004**, *126*, 12730−12731.
(32) Tao, A.; Kim, F.; Hess, C.; Goldberger, J.; He, R.; Sun, Y.; Xia, Y.; Yang, P. *Nano Lett.* **2003**, *3*, 1229−1233.
(33) Hanarp, P.; Kall, M.; Sutherland, D. S. *J. Phys. Chem. B* **2003**, *107*, 5768−5772.
(34) Gluodenis, M.; Foss, C. A., Jr. *J. Phys. Chem. B* **2002**, *106*, 9484−9489.
(35) Nikoobakht, B.; El-Sayed, M. A. *J. Phys. Chem. A* **2003**, *107*, 3372−3378.
(36) Taton, T. A.; Mirkin, C. A.; Letsinger, R. L. *Science* **2000**, *289*, 1757−1760.
(37) Kim, Y.; Johnson, R. C.; Hupp, J. T. *Nano Lett.* **2001**, *1*, 165−167.
(38) Thanh, N. T. K.; Rosenzweig, Z. *Anal. Chem.* **2002**, *74*, 1624−1628.
(39) Nicewarmer-Pena, S. R.; Freeman, R. G.; Reiss, B. D.; He, L.; Pena, D. J.; Walton, I. D.; Cromer, R.; Keating, C. D.; Natan, M. J. *Science* **2001**, *294*, 137−141.
(40) Kneipp, K.; Haka, A. S.; Kneipp, H.; Badizadegan, K.; Yoshizawa, N.; Boone, C.; Shafer-Peltier, K. E.; Motz, J. T.; Dasari, R. R.; Feld, M. S. *Appl. Spectrosc.* **2002**, *56*, 150−154.
(41) McFarland, A. D.; Van Duyne, R. P. *Nano Lett.* **2003**, *3*, 1057−1062.
(42) Grubisha, D. S.; Lipert, R. J.; Park, H. Y.; Driskell, J.; Porter, M. D. *Anal. Chem.* **2003**, *75*, 5936−5943.
(43) Shafer-Peltier, K. E.; Haynes, C. L.; Glucksberg, M. R.; Van Duyne, R. P. *J. Am. Chem. Soc.* **2003**, *125*, 588−593.
(44) Obare, S. O.; Hollowell, R. E.; Murphy, C. J. *Langmuir* **2002**, *18*, 10407−10410.
(45) Hirsch, L. R.; Jackson, J. B.; Lee, A.; Halas, N. J.; West, J. L. *Anal. Chem.* **2003**, *75*, 2377−2381.
(46) Roll, D.; Malicka, J.; Gryczynski, I.; Gryczynski, Z.; Lakowicz, J. R. *Anal. Chem.* **2003**, *75*, 3106−3113.

(47) Keating, C. D.; Kovaleski, K. M.; Natan, M. J. *J. Phys. Chem. B* **1998**, *102*, 9404−9413.
(48) Maxwell, D. J.; Emory, S. R.; Nie, S. *Chem. Mater*. **2001**, *13*, 1082−1088.
(49) Gearheart, L.; Ploehn, H. J.; Murphy, C. J. *J. Phys. Chem. B* **2001**, *105*, 12609−12615.
(50) Cao, Y.; Jin, R.; Mirkin, C. A. *Science* **2002**, *297*, 1536−1540.
(51) Culha, M.; Stokes, D.; Allain, L. R.; Vo-Dinh, T. *Anal. Chem*. **2003**, *75*, 6196−6201.
(52) Templeton, A. C.; Pietron, J. J.; Murray, R. W.; Mulvaney, P. *J. Phys. Chem. B* **2000**, *104*, 564−570.
(53) Xu, X.-H. N.; Brownlow, W. J.; Kyriacou, S. V.; Wan, Q.; Viola, J. J. *Biochemistry* **2004**, *43*, 10400−10413.
(54) Cognet, L.; Tardin, C.; Boyer, D.; Choquet, D.; Tamarat, P.; Lounis, B. *Proc. Natl. Acad. Sci. U.S.A.* **2003**, *100*, 11350−11355.
(55) Bailey, R. C.; Nam, J.-M.; Mirkin, C. A.; Hupp, J. T. *J. Am. Chem. Soc*. **2003**, *125*, 13541−13547.
(56) Nam, J.-M.; Thaxton, C. J.; Mirkin, C. A. *Science* **2003**, *301*, 1884−1886.
(57) Xu, X.-H. N.; Chen, J.; Jeffers, R. B.; Kyriacou, S. *Nano Lett*. **2002**, *2*, 175−182.
(58) Nath, N.; Chilkoti, A. *Anal. Chem*. **2002**, *74*, 504−509.
(59) Sokolov, K.; Chumanov, G.; Cotton, T. M. *Anal. Chem*. **1998**, *70*, 3898−3905.
(60) Malicka, J.; Gryzczynski, I.; Lakowicz, J. R. *Anal. Chem*. **2003**, *75*, 4408−4414.
(61) Parfenov, A.; Gryzczynski, I.; Malicka, J.; Geddes, C. D.; Lakowicz, J. R. *J. Phys. Chem. B* **2003**, *107*, 8829−8833.
(62) Lakowicz, J. R.; Geddes, C. D.; Gryzczynski, I.; Malicka, J.; Gryzczynski, Z.; Aslan, K.; Lukomski, J.; Matveera, E.; Zhang, J.; Badugn, R.; Huang, J. *J. Fluorescence* **2004**, *14*, 425−441.
(63) Hirsch, L. R.; Stafford, R. J.; Bankson, J. A.; Rivera, B.; Hazle, J. D.; Halas, N. J.; West, J. L. *Proc. Natl. Acad. Sci. U.S.A.* **2003**, *100*, 13549−13554.
(64) Yu, Y.-Y.; Chang, E.-S.; Lee, C.-L.; Wang, C. R. C. *J. Phys. Chem. B* **1997**, *101*, 6661−6664.
(65) Hu, J.; Odom, T. W.; Lieber, C. M. *Acc. Chem. Res*. **1999**, *32*, 435−445.
(66) Jana, N. R.; Gearheart, L. A.: Murphy, C. J. *Chem. Commun*. **2001**, 617−618.
(67) Jana, N. R.; Gearheart, L.; Murphy, C. J. *J. Phys. Chem. B* **2001**, *105*, 4065−4067.
(68) Murphy, C. J.; Jana, N. R. *Adv. Mater*. **2002**, *14*, 80−82.
(69) Sun, Y.; Mayers, D.; Herricks, T.; Xia, Y. *Nano Lett.* **2003**, *3*, 955−960.
(70) Nikoobakht, B.; El-Sayed, M. A. *Chem. Mater*. **2003**, *15*, 1957−1962.
(71) Liu, M.; Guyot-Sionnest, P. *J. Phys. Chem. B* **2004**, *108*, 5882−5888.
(72) Sau, T. K.; Murphy, C. J. *Langmuir* **2004**, *20*, 6416−6420.
(73) Walter, E. C.; Murray, B. J.; Favier, F.; Kaltenpoth, G.; Grunze, M.; Penner, R. M. *J. Phys. Chem. B* **2002**, *106*, 11407−11411.
(74) Filankembo, A.; Giorgio, S.; Lisiecki, I.; Pileni, M.-P. *J. Phys. Chem. B* **2003**, *107*, 7492−7500.
(75) Sun, Y.; Xia, Y. *Science* **2002**, *298*, 2176−2179.
(76) Sun, Y.; Xia, Y. *Adv. Mater*. **2002**, *12*, 1875−1881.
(77) Jin, R.; Cao, Y. C.; Han, E.; Metraux, G. S.; Schatz, G. C.; Mirkin, C. A. *Nature* **2003**, *425*, 487−490.
(78) Jin, R.; Cao, Y.; Mirkin, C. A.; Kelly, K. L.; Schatz, G. C.; Zheng, J. *Science* **2001**, *294*, 1901−1904.
(79) Puntes, V. F.; Krishnan, K. M.; Alivisatos, A. P. *Science* **2001**, *291*, 2115−2117.
(80) Milliron, D. J.; Hughes, S. M.; Cui, Y.; Manna, L.; Li, J.; Wang, L.-W.; Alivisatos, A. P. *Nature* **2004**, *430*, 190−195.
(81) Dujardin, E.; Hsin, L.-B.; Wang, C. R. C.; Mann, S. *Chem. Commun.* **2001**, 1264−1265.
(82) Mbindyo, J. K. N.; Reiss, B. D.; Martin, B. R.; Keating, C. D.; Natan, M. J.; Mallouk, T. E. *Adv. Mater*. **2001**, *13*, 249−254.
(83) Van Bruggen, M. P. B.; Lekkerkerker, H. N. W. *Langmuir* **2002**, *18*, 7141−7145.
(84) Li, L. S.; Alivisatos, A. P. *Adv. Mater*. **2003**, *15*, 408−411.
(85) Jana, N. R.; Gearheart, L. A.; Obare, S. O.; Johnson, C. J.; Edler, K. J.; Mann, S.; Murphy, C. J. *J. Mater. Chem.* **2002**, *12*, 2909−2912.
(86) Caswell, K. K.; Wilson, J. N.; Bunz, U. H. F.; Murphy, C. J. *J. Am. Chem. Soc*. **2003**, *125*, 13914−13915.
(87) Mokari, T.; Rothenberg, E.; Popov, I.; Costi, R.; Banin, U. *Science* **2004**, *304*, 1787−1790.
(88) Yu, J.-S.; Kim, J. Y.; Lee, S.; Mbindyo, J. K. N.; Martin, B. R.; Mallouk, T. E. *Chem Commun*. **2000**, 2445−2446.
(89) Glotzer, S. C. *Science* **2004**, *306*, 419−420.
(90) Pacholski, C.; Kornowski, A.; Weller, H. *Angew. Chem., Int. Ed. Engl*. **2004**, *43*, 4774−4777.
(91) Shah, P. S.; Hanrath, T.; Johnston, K. P.; Korgel, B. A. *J. Phys. Chem. B* **2004**, *108*, 9574−9587.
(92) Ding, Y.; Wang, Z. L. *J. Phys. Chem. B* **2004**, *108*, 12280−12291.
(93) Scott, R. W. J.; Wilson, O. M.; Crooks, R. M. *J. Phys. Chem. B* **2005**, *109*, 692−704.
(94) Jana, N. R.; Gearheart, L.; Murphy, C. J. *Adv. Mater.* **2001**, *13*, 1389−1393.
(95) Jana, N.; Gearheart, L.; Murphy, C. J. *Langmuir* **2001**, *17*, 6782−6786.
(96) Johnson, C. J.; Dujardin, E.; Davis, S. A.; Murphy, C. J.; Mann, S. *J. Mater. Chem*. **2002**, *12*, 1765−1770.
(97) Busbee, B. D.; Obare, S. O.; Murphy, C. J. *Adv. Mater*. **2003**, *15*, 414−416.
(98) Sau, T. K.; Murphy, C. J *J. Am. Chem. Soc*. **2004**, *126*, 8648−8649.
(99) Gole, A.; Murphy, C. J. *Chem. Mater*. **2004**, *16*, 3633−3640.
(100) Nikoobakht, B.; El-Sayed, M. A. *Langmuir* **2001**, *17*, 6368−6374.
(101) Filankembo, A.; Pileni, M. P. *J. Phys. Chem. B* **2000**, *104*, 5865−5868.
(102) Caswell, K. K.; Bender, C. M.; Murphy, C. J. *Nano Lett.* **2003**, *3*, 667−669.
(103) Gai, P. L.; Harmer, M. A. *Nano Lett.* **2002**, *2*, 771−774.
(104) Gao, J.; Bender, C. M.; Murphy, C. J. *Langmuir* **2003**, *19*, 9065−9070.
(105) Sau, T. K.; Murphy, C. J. *Langmuir* **2005**, *21*, 2923−2929.
(106) Anacker, E. W. In *Cationic Surfactants*; Jungermann, E., Ed.; Marcel Dekker: New York, 1970.
(107) Magnussen, O. M.; Ocko, B. M.; Wang, J. X.; Adzic, R. R. *J. Phys. Chem*. **1996**, *100*, 5500−5508.
(108) Ocko, B. M.; Magnussen, O. M.; Wang, J. X.; Wandlowski, T. *Phys. Rev. B* **1996**, *53*, R7654−R7657.
(109) Wang, J. X.; Marinkovic, N. S.; Adzic, R. R. *Colloids Surf. A* **1998**, *134*, 165−171.
(110) Shi, Z. C.; Lipkowski, J.; Mirwald, S.; Pettinger, B. *J. Chem. Soc., Faraday Trans*. **1996**, *92*, 3737−3746.
(111) Zou, S. Z.; Gao, X. P.; Weaver, M. J. *Surf. Sci*. **2000**, *452*, 44−57.
(112) Perez-Juste, J.; Liz-Marzan, L. M.; Carnie, S.; Chan, D. Y. C.; Mulvaney, P. *Adv. Funct. Mater.* **2004**, *14*, 571−579.
(113) Diao, J.; Gall, K.; Dunn, M. L. *Nature Mater.* **2003**, *2*, 656−660.
(114) van der Zande, B. M. I.; Pages, L.; Hikmet, R. A. M.; van Blaaderen, A. *J. Phys. Chem. B* **1999**, *103*, 5761−5767.
(115) Artemyer, M.; Muller, B.; Woggon, U. *Nano Lett.* **2003**, *3*, 509−512.
(116) Thomas, K. G.; Barazzouk, S.; Ipe, B. I.; Joseph, S. T. S.; Kamat, P. V *J. Phys. Chem. B* **2004**, *108*, 13066−13068.
(117) van der Zande, B. M. I.; Koper, G. J. M.; Lekkerkerker, H. N. W. *J. Phys. Chem. B* **1999**, *103*, 5754−5760.
(118) Varghese, S.; Narayanankutty, S.; Bastiaansen, C. W. M.; Crawford, G. P.; Broer, D. J. *Adv. Mater*. **2004**, *16*, 1600−1605.
(119) Raschke, G.; Kowarik, S.; Franzl, T.; Sonnichsen, C.; Klar, T. A.; Feldmann, J.; Nichtl, A.; Kurzinger, K. *Nano Lett*. **2003**, *3*, 935−938.
(120) Mock, J. J.; Smith, D. R.; Schultz, S. *Nano Lett*. **2003**, *3*, 485−491.
(121) Prikulis, J.; Svedberg, F.; Kall, M.; Enger, J.; Ramser, K.; Goksor, M.; Hanstorp, D. *Nano Lett.* **2004**, *4*, 115−118.
(122) Sonnichsen, C.; Alivisatos, A. P. *Nano Lett*. **2005**, *5*, 301−304.
(123) Maier, S. A.; Kik, P. G.; Atwater, H. A. *Appl. Phys. Lett.* **2002**, *81*, 1714−1716.
(124) Gabriel, J.-C. P.; Davidson, P. *Top. Curr. Chem*. **2003**, *226*, 119−172.
(125) Caruso, F. *Top. Curr. Chem*. **2003**, *227*, 145−168.
(126) Gole, A.; Murphy, C. J. *Chem. Mater*. **2005**, *17*, 1325−1330.
(127) Orendorff, C. J.; Hankins, P.; Murphy, C. J. *Langmuir* **2005**, *21*, 2022−2026.
(128) Stoeva, S. I.; Prasad, B. L. V.; Uma, S.; Stoimenov, P. K.; Zaikovski, V.; Sorensen, C. M.; Klabunde, K. J. *J. Phys. Chem. B* **2003**, *107*, 7441−7448.
(129) Dujardin, E.; Hsin, L.-B.; Wang, C. R. C.; Mann, S. *Chem. Commun.* **2001**, 1264−1265.
(130) Love, C. J.; Urbach, A. R.; Prentiss, M. G.; Whitesides, G. M. *J. Am. Chem. Soc*. **2003**, *125*, 12696−12697.
(131) Greenwood, N. N.; Earnshaw, A. *Chemistry of the Elements*, 2nd ed.; Butterworth-Heinemann: Oxford, UK, 1997.
(132) Rodriguez-Gonsalez, B.; Sanchez-Iglesias, A.; Giersig, M.; Liz-Marzan, L. M. *Faraday Discuss*. **2004**, *125*, 133−144.
(133) Jana, N. R.; Gearheart, L.; Obare, S. O.; Murphy, C. J. *Langmuir* **2002**, *18*, 922−927.
(134) Hardikar, V. V.; Matijevic, E. *J. Colloid Interface Sci.* **2000**, *221*, 133−136.
(135) Mulvaney, P.; Liz-Marzan, L. M.; Giersig, M.; Ung, T. *J. Mater. Chem*. **2000**, *10*, 1259−1270.

(136) Lu, Y.; Yin, Y. D.; Li, X. Z.; Xia, Y. *Nano Lett.* **2002**, *2*, 785−788.
(137) Mine, E.; Yamada, A.; Kobayashi, Y.; Konno, M.; Liz-Marzan, L. M. *J. Colloid Interface Sci.* **2003**, *264*, 385−390.
(138) Obare, S. O.; Jana, N. R.; Murphy, C. J. *Nano Lett.* **2001**, *1*, 601−603.
(139) Andrew, P.; Barnes, W. L. *Science* **2004**, *306*, 1002−1005.
(140) Creighton, J. A.; Eadon, D. G. *J. Chem. Soc., Faraday Trans.* **1991**, *87*, 3881−3891.
(141) Prodan, E.; Radloff, C.; Halas, N. J.; Norlander, P. *Science* **2003**, *302*, 419−422.
(142) Aizpurua, J.; Hanarp, P.; Sutherland, D. S.; Kall, M.; Bryant, G. W.; Garcia de Abajo, F. J. *Phys. Rev. Lett.* **2003**, *90*, 57401.
(143) Storhoff, J. J.; Elghanian, R.; Mucic, R. C.; Mirkin, C. A.; Letsinger, R. L. *J. Am. Chem. Soc.* **1998**, *120*, 1959−1964.
(144) Lin, S. Y.; Liu, S. W.; Lin, C. W.; Chen, C. H. *Anal. Chem.* **2002**, *74*, 330−335.
(145) Liu, J. W.; Lu, Y. *Anal. Chem.* **2004**, *76*, 1627−1632.
(146) Kreibig, U.; Vollmer, M. *Optical Properties of Metal Clusters*; Springer: Berlin, 1995.
(147) Lazarides, A. A.; Schatz, G. C. *J. Phys. Chem. B* **2000**, *104*, 460−467.
(148) Su, K.-H.; Wei, Q.-H.; Zhang, X.; Mock, J. J.; Smith, D. R.; Schultz, S. *Nano Lett.* **2003**, *3*, 1087−1090.
(149) Haes, A. J.; Chang, L.; Klein, W. L.; Van Duyne, R. P. *J. Am. Chem. Soc.* **2005**, *127*, 2264−2271.
(150) Vidal, F. J. G.; Pendry, J. B. *Phys. Rev. Lett.* **1996**, *77*, 1163−1166.
(151) Wang, D. S.; Kerker, M. *Phys. Rev. B* **1981**, *24*, 1777−1790.
(152) Markel, V. A.; Shalaev, V. M.; Zhang, P.; Huynh, W.; Tay, L.; Haslett, T. L.; Moskovits, M. *Phys. Rev. B* **1999**, *59*, 10903−10909.
(153) Su, K.-H.; Wei, Q.-H.; Zhang, X.; Mock, J. J.; Smith, D. R.; Schultz, S. *Nano Lett.* **2003**, *3*, 1087−1090.
(154) Atay, T.; Song, J-. H.; Murmikko, A. V. *Nano Lett.* **2004**, *4*, 1627−1731.
(155) Fromm, D. P.; Sundaramurthy, A.; Schuck, P. J.; Kino, G.; Moerner, W. E. *Nano Lett.* **2004**, *4*, 957−961.
(156) Schatz, G. C. *Acc. Chem. Res.* **1984**, *17*, 370−376.
(157) Gersten, J. I. *J. Chem. Phys.* **1980**, *72*, 5779−5780.
(158) Tao, A.; Kim, F.; Hess, C.; Goldberger, J.; He, R.; Sun, Y.; Xia, Y.; Yang, P. *Nano Lett.* **2003**, *3*, 1229−1323.
(159) Jeong, D. H.; Zhang, Y. X.; Moskovits, M. *J. Phys. Chem. B* **2004**, *108*, 12724−12728.
(160) Yao, J. L.; Pan, G. P.; Xue, K. H.; Wu, D. Y.; Ren, B.; Sun, D. M.; Tang, J.; Xu, X.; Tian, Z. Q. *Pure Appl. Chem.* **2000**, *72*, 221−228.
(161) Nikoobakht, B.; Wang, J.; El-Sayed, M. A. *Chem. Phys. Lett.* **2002**, *366*, 17−23.
(162) Nikoobakht, B.; El-Sayed, M. A. *J. Phys. Chem. A* **2003**, *107*, 3372−3378.
(163) Orendorff, C. J.; Gearheart, L.; Jana, N. R.; Murphy, C. J. *Chem. Phys. Chem.*, submitted.
(164) Orendorff, C. J.; Gole, A.; Sau, T. K.; Murphy, C. J. *Anal. Chem.* **2005**, *77*, 3261−3266.
(165) Shchegrov, A. V.; Novikov, I. V.; Maradudin, A. A. *Phys. Rev. Lett.* **1997**, *78*, 4269−4272.
(166) Holland, W. R.; Hall, D. G. *Phys. Rev. B* **1983**, *27*, 7765−7768.
(167) Kume, T.; Nakagawa, N.; Yamamoto, K. *Solid State Commun.* **1995**, *93*, 171−175.
(168) Lyon, L. A.; Musick, M. D.; Natan, M. J. *Anal. Chem.* **1998**, *70*, 5177−5183.
(169) Lyon, L. A.; Pena, D. J.; Natan, M. J. *J. Phys. Chem. B* **1999**, *103*, 5826−5831.
(170) Hutter, E.; Cha, S.; Liu, J.-F.; Park, J.; Yi, J.; Fendler, J. H.; Roy, D. *J. Phys. Chem. B* **2001**, *105*, 8−12.